International Journal of Thermophysics, Vol. 16, No. 3, 1995

Experimental Study of Phase Transitions in Mercury[1]

V. F. Kozhevnikov,[2,3] D. I. Arnold,[4] and S. P. Naurzakov[4]

The results of sound velocity measurements in mercury, performed at temperatures from 300 up to 2050 K and pressures from 30 up to 1900 bar by a precise pulsed phase-sensitive technique for a frequency of 10 MHz, are presented. The explored range of state parameters includes liquid and gaseous phases, the coexistence curve up to the critical point, and the supercritical region. The data obtained indicate the existence of two first-order phase transitions in mercury that take place in the vapor near saturation and in the supercritical fluid. The positions of the critical points of these transitions were estimated. An interpretation of the observed phenomena is given: It leads to the new approach to the nature of the critical point of liquid–gas transition in mercury. It is shown also that the fourth derivative of the thermodynamic potential of mercury has a special feature in the metal–nonmetal transition region.

KEY WORDS: clusters; critical point; mercury; metal–nonmetal transition; phase transition; sound velocity.

1. INTRODUCTION

Fifty years ago Landau and Zeldovich [1] proposed that the high-temperature part of the phase diagram for low-boiling liquid metals (such as mercury) may differ from the diagram for Guggenheim dielectric liquids; the former may contain an additional phase transition of the first order connected with the metal–nonmetal (MNM) transition. Much attention was given by Mott [2] to electronic properties of condensed metals near the MNM transition.

Pioneer experimental works [3, 4] showed that the MNM transition in mercury occurs at a density of about $9\,\mathrm{g\cdot cm^{-3}} \approx 1.5\,\rho_c$, where

[1] Invited paper presented at the Twelfth Symposium on Thermophysical Properties, June 19–24, 1994, Boulder, Colorado, U.S.A.

[2] Moscow Aviation Institute, 125871 Moscow, Russia.

[3] To whom correspondence should be addressed.

[4] Russian Research Centre "Kurchatov Insitute," 123182 Moscow, Russia.

0195-928X/95/0500-0619$07.50/0

$\rho_c = 5.8\ \mathrm{g \cdot cm^{-3}}$, the density in the critical point (the other mercury critical parameters are $T_c = 1751$ K, $P_c = 1673$ bar [5]). This result has been corroborated by data on the Hall effect [6], NMR [7], and optical absorption [8]. It was shown also that the mean diameter of the mercury phase diagram is not rectilinear: it bends toward the liquid branch ("positive" direction) at temperatures from $0.8\ T_c$ to the close vicinity of the critical point [4, 5, 9]. The cesium mean diameter, however, bends in the "negative" direction at $T \geqslant 0.6 T_c$ [10]. Another feature of the mercury equation of state concerns the value of $r = \rho_t/\rho_c$ (ρ_t, triple point density). For Guggenheim liquids $r_g \approx 2.7$ and for alkali metals $r_a \approx 4.5$; this is usually explained by more long-range character of the metallic bond as compared to van der Waals interaction. But for mercury, that is, the metallic liquid in the main part of the phase diagram, $r_m \approx 2.3$.

It was shown also that strong anomalies occur in the behavior of the thermopower S and the real part of the dielectric constant ε_1. The thermopower has sharp maxima in the vapor phase near the saturation line at high temperatures and along the critical isochore at pressure less than 1900 bar [5, 11, 12]. The real part of dielectric constant shows abrupt upward deviations from normal Clausius–Mosotti behavior in the vapor phase near saturation and at supercritical temperatures [13–15] at optical frequencies.

A physical reason for the thermopower anomalies was not found (see, e.g., Ref. 16). The results on ε_1 are interpreted by authors as the appearance of a number of large clusters like droplets. At present, there are two theoretical approaches to the cluster interpretation. The first is a "plasma transition" (see, e.g., Refs. 16 and 17), and the second the "exitonic transition" of Turkevich and Cohen [18]. The qualitative difference between clusters in plasma and exitonic models is the presence or absence of charge.

So the high-temperature part of the mercury phase diagram is very complicated. The main purpose of this work is to clarify the situation by means of precise measurements of the sound velocity (SV) U; it is connected directly with the adiabatic compressibility $K_s \equiv \rho^{-1}(\partial\rho/\partial P)_s = \rho^{-1}U^{-2}$, the susceptibility that can be studied in detail at state parameters of interest.

2. EXPERIMENTS

For the first time the SV in mercury up to supercritical state parameters (at $T < 1900$ K and $P < 200$ bar) had been measured by Suzuki et al. [19] with a pulsed transmission/echo technique. More precise techniques were used in Refs. 20 and 21, but in a narrower temperature range: up to 1000 and 1500 K, respectively.

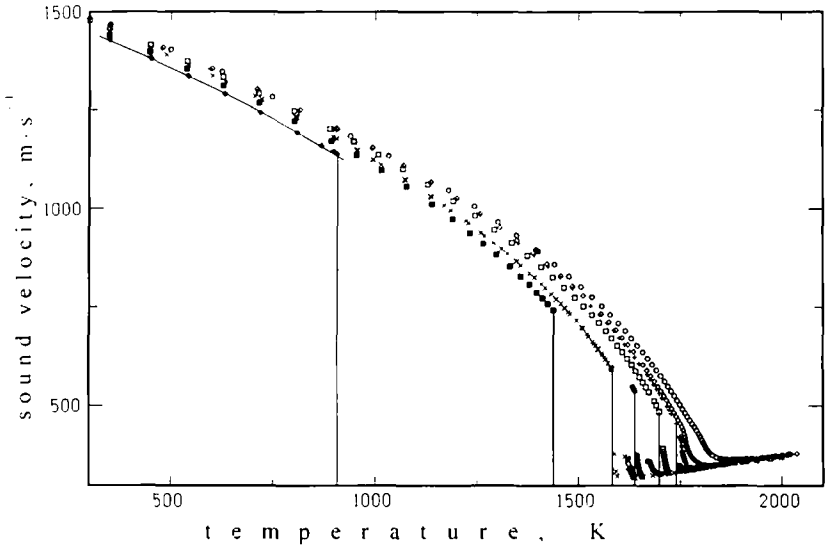

Fig. 1. Overview of the data on sound velocity in mercury. Isobars: (◆) 30 bar; (■) 600 bar; (×) 1000 bar; (●) 1200 bar; (□) 1400 bar; (+) 1600 bar; (·) 1700 bar; ( ) 1900 bar. Solid line, isobar 50 bar [21]. Vertical lines mark the liquid-gas transition.

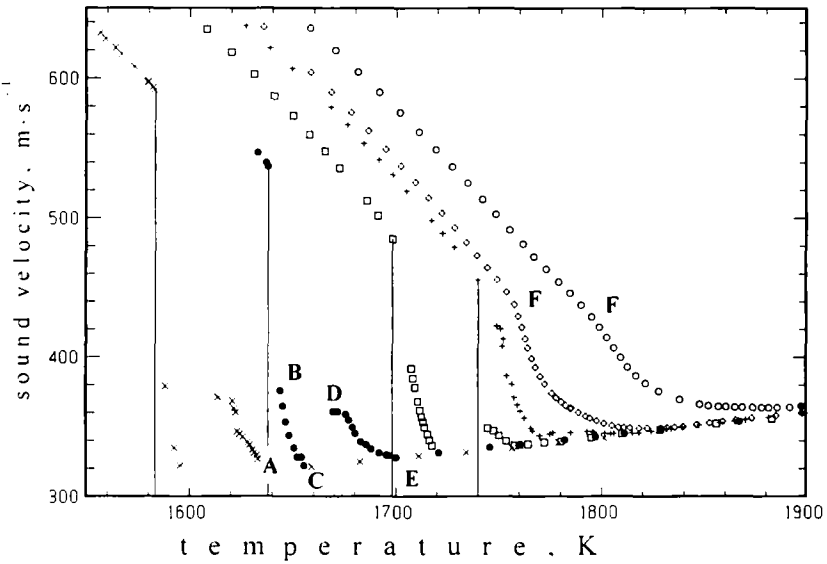

Fig. 2. Sound velocity in the critical point area of mercury. Symbols, see the legend to Fig. 1; points A–F, see text.

In this work the measurements were performed by a precise pulsed phase-sensitive technique [22, 23] at 10 MHz. The essence of the technique consists in *comparison of phases* of high-frequency oscillations of *radio-pulses first propagated* through the sample *and first reflected* in a buffer rod. So, this technique combines the advantages of both classical methods of SV measurements: the ability to reach the highest temperatures of echo-pulsed method (see, e.g., Ref. 19) and the high accuracy of phase techniques [24].

The accuracy of measurement of the variation of ultrasonic-pulse propagation time through the sample of 2.5-mm length was 1 ns. The temperature variation along the sample $\Delta T/T$ was of the order 10^{-3}. Pressure was measured with an uncertainty of 2 bar. A more detailed description of the cell and the setup employed can be found in Refs. 25 and 26.

SV was measured along eight isobars, 30–1900 bar, at temperatures both rising and falling within the range from 300 up to 2050 K. The overview of data obtained is shown in Fig. 1, whereas the data near and above the critical point are shown on a large scale in Fig. 2.

3. DISCUSSION

A sharp jump in isobaric dependence $U(T)$ at pressures less then 1700 bar was observed. The temperatures of the jumps agree well with vapor pressure data of the Marburg group [5] so that these jumps mark the liquid–vapor phase transition. For $U(T)$ at pressures of 1700 and 1900 bar no jumps were observed and the propagated signal was stable over the isobar, therefore the critical pressure of mercury is somewhat lower than 1700 bar, in agreement with critical parameters derived from PVT experiments [5, 9]. The SV data obtained for the liquid phase agree well with reliable literature data [20, 21]. For example, the data of the Marburg group [21] for the 50-bar isobar are shown in Fig. 1.

One can see in Fig. 2 that the results contain three kind of peculiarities: (i) an abnormal dependence of $U(T)$ in the vapor phase near saturation; (ii) a break point on supercritical isobars (marked by F), that are located along the isochore $\rho = \rho_c$ (where SV of dielectric liquids has a minimum [27]); and (iii) an absence of a minimum in $U(T)$ dependence near the critical point (for dielectric liquids such a minimum is always observed [27]).

All subcritical isobars showed in Fig. 2 contain characteristic points. For convenience they are marked on the 1200-bar isobar only. Point A and the vertical line correspond to the liquid–gas transition temperature, and the ordinate of point A corresponds to the expected value of SV in saturated vapor: it is the point on the normal temperature dependence of SV for mercury vapor (see below); B is a point near the first maximum;

C is a minimum point; D is the second maximum point; E is the end point of the abnormal part of the isobar. The description of points B and D is conventional; we may call them points of discontinuities as well.

At temperature $T > T_E$ we call the $U(T)$ dependence "normal." The characteristic feature of SV data for normal mercury vapor is their pressure independence. From the comparison of the normal part $U(T)$ with one- and two-atomic ideal-gas dependencies, it can be shown that the normal component of mercury vapor consists mainly of atoms [26].

In contrast, on the abnormal part of the isobars the propagated signal is very sensitive to any changes of P or T. The absence of experimental points in sections A–B and C–D is associated with strong instability of the signal, which does not allow us to carry out any measurements.

As follows from the data obtained, when the pressure increases the amplitude of the D maximum falls, whereas the amplitude of the B maximum rises, and the signal becomes more stable.

Founding our arguments upon either of the cluster transition ideas (for our case it is irrelevant whether the clusters are charged or not), we may suggest the following qualitative interpretation of the observed peculiarities. Let us assume that there are two cluster transitions in mercury vapor and that in each of them only one kind of cluster is born. As shown below, we may expect that the mass density of the B clusters is about the critical density $\rho_B \approx \rho_c \approx 6\ \mathrm{g \cdot cm^{-3}}$, whereas the density of the D clusters is about half of that of the B clusters.

It should be noted that it is impossible to explain the abnormal part of the subcritical isobars as due to a temperature gradient along the sample, that might lead to the appearance of a heterogeneous system like a fog: liquid droplets in vapor at saturation. First of all, the temperature interval of the abnormal part of the isobars is too large. Moreover, for such a system SV must always be less than for the homogeneous vapor [28], whereas SV in mercury at the abnormal region is higher compared to the normal, that is, homogeneous vapor. But such an increase in SV is possible in the heterogeneous system consisting of stable large clusters and the normal gas.

When the critical point is approached the number of clusters appearing at the transition point has to rise for both models. Hence, the greater the difference between the cluster density and the normal vapor density, the more the SV in the heterogeneous system differs from that in the homogeneous vapor, and vice versa: The more the normal vapor density approaches the cluster density, the less is the influence of clusters on the behavior of the SV of the system.

Therefore, with this assumption, one can expct the behavior of SV as in the experiment.

As can be seen from Fig. 2, the B transition is very close to the liquid–gas transition, so we can expect that saturated mercury vapor at high pressure is a heterogeneous system of the normal component and heavy B clusters. The assumption that the B transition does not end in the critical point may be used to explain the appearance of break points F on

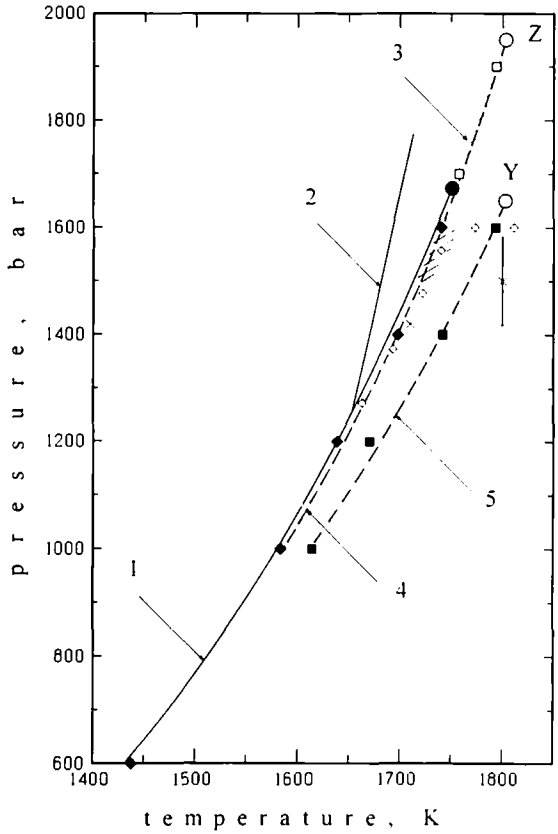

Fig. 3. Phase diagram of mercury. (1) Coexistence curve; (2) isochore near the MNM transition ($\rho = 9\,\mathrm{g \cdot cm^{-3}}$); (3) area of the thermopower maximum locations [5, 11, 12]; (4, 5) curves of the B and D transitions, respectively. (●) Liquid–gas critical point; (◆) position of A points; (■) positions of D points; (□) positions of F points; (Z and Y) approximate positions of the B and D transition end points (critical points), respectively; (×) positions of the dielectric abnormality at 0.6 eV [3]; (◇) positions of the dielectric abnormality at 1.9 eV [14].

supercritical isobars. Thus we believe that the F points at $P > P_c$ are the same as the B points at $P < P_c$.

The P–T phase diagram of mercury is shown in Fig. 3. The curves of the B and D transitions are shown by dashed lines. We cannot say where the beginnings of these curves are because the SV measurements in the gas phase were not carried out at pressures less then 1000 bar. As can be seen from Fig. 2, in the last experimental points on the curves of the B and D transitions (at pressure of 1900 and 1600 bar, respectively), the observed SV peculiarities have almost disappeared. Hence these experimental points are like a critical point of the corresponding cluster-transition line, where the difference between the cluster and the normal vapor component densities vanishes. Approximate positions of these end points are marked by Z and Y; their coodinates are about (1800 K, 1950 bar) and (1800 K, 1650 bar), respectively. The last experimental points on the curve of B and D transitions are on isochores at about the critical density and $3.3\ \mathrm{g \cdot cm^{-3}}$, respectively, which is why such values of density for B and D clusters have been suggested above.

Concerning the absence of a minimum in the $U(T)$ dependence near the liquid–gas critical point, we believe that the closeness of the vapor–liquid critical point to the curve of the cluster transition might lead to abnormal critical behavor of SV in mercury, such as a narrowing of the region where SV minima can be observed.

4. SUMMARY

In contrast with dielectric liquids, where the rectilinear diameter rule is valid, the appearance of a large number of heavy clusters in mercury vapor at high temperatures must lead to the asymmetry of the mercury ρ–T phase diagram with positive curvature of its mean diameter. Furthermore, in such case one can expect that the fluid density at the critical point will be higher than in the case of absence of clusters, that is, at a smaller value of r_m (see above). Hence the suggested interpretation of SV peculiarities may explain the observed features of the mercury equation of state.

Maxima of the thermopower occur near the high-temperature part of the B transition curve. The locations of the ε_1 abnormalities [13, 14] are shown in Fig. 3 by crosses and diamonds. The marked uncertainty of the location of ε_1 abnormality has been taken from Ref. 29. Taking into account the errors of these and our data, they agree well with each other: Some points belong to the B transitions curve, and the others to the D transitions curve. Thus all peculiarities of S, ε_1, and SV are located near the B and D curves in Fig. 3. Hence one can expect that they all have the same nature.

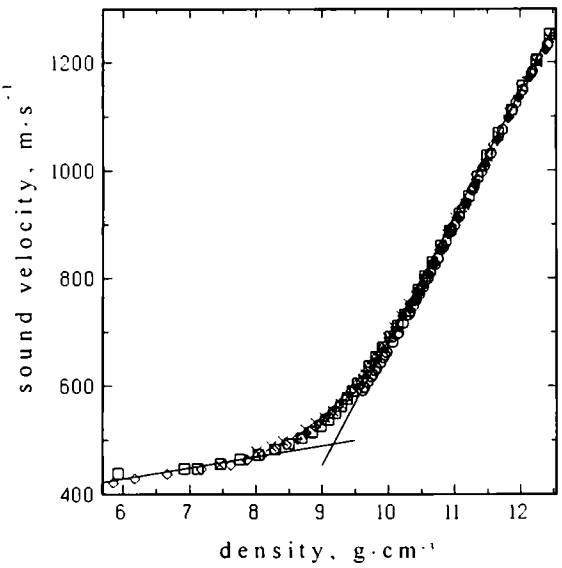

Fig. 4. The density dependence of mercury sound velocity at $\rho \geq \rho_c$ and pressures of (◆) 600 bar, (○) 1000 bar, (+) 1400 bar, (×) 1600 bar, (□) 1700 bar, and (·) 1900 bar.

Finally, we have to return to the question about the MNM transition in mercury. In Fig. 4 the SV data versus density are presented; the Marburg group data on equation of state [5] were used. The most surprising result is that practically a single density dependence can be used for all SV data obtained in the whole range of the mercury liquid phase, in contrast with the Guggenheim liquids [30] and alkali metals [10]. As one can see from Fig. 4 this dependence can be roughly approximated by two straight lines intersecting at density near 9 g·cm^{-3}, where the MNM transition occurs. That is, in the region of the MNM transition the fastest variation of the slope of $U(\rho)$ dependence, i.e., a maximum of the second derivative $d^2U/d\rho^2$ or a maximum of the fourth derivative of the internal energy, is observed [note that $U^2 = (\partial P/\partial \rho)_s \equiv v^2(\partial^2 E/\partial v^2)_s$, where E is the specific internal energy and $v = 1/\rho$ is the specific volume]. An analogous result has been found by Suzuki et al. [19].

In conclusion, it should be noted that we certainly do not consider the suggested interpretation of the observed peculiarities in the behavior of the mercury vapor to be the only one possible. In any case, additional detailed experimental investigations in the regions of the B and D curves, as well as near the critical point of mercury, are required for construction of a quantitative model of the observed phenomena.

ACKNOWLEDGMENTS

Authors thank Dr. A. A. Borzhievsky, Mr. N. A. Naumenko, and Mr. E. V. Grodzinskii for help in preparing the experiment. We are grateful to Professor F. Hensel, Dr. H. Uchtmann, and Dr. C. Pilgrim for stimulating discussion. The work was supported by Russian Foundation of Fundamental Researches Grant 94-02-03656.

REFERENCES

1. L. Landau and I. Zeldovich, *Acta Phys. Chem. USSR* **18**:1940 (1943).
2. N. Mott, *Metal-Insulator Transitions* (Taylor & Francis, London, 1974).
3. F. Hensel and E. U. Frank, *Ber. Bunsenges. Phys. Chem.* **70**:1154 (1966).
4. I. K. Kikoin and A. P. Senchenkov, *Fizika Metallov i Metallovedenie* **24**:843 (1967) (in Russian).
5. W. Gotzlaff, G. Shonherr, and F. Hensel, *Z. Phys. Chem. N.F.* **156**:219 (1988); W. Gotzlaff, Thesis (Marburg University, Marburg, 1988).
6. U. Even and J. Jortner, *Phys. Rev. Lett.* **28**:31 (1972).
7. W. W. Warren, Jr., and F. Hensel, *Phys. Rev. B* **26**:5980 (1982).
8. M. Yao, W. Hayami, and H. Endo, *J. Non-Crustall. Solids* **117/118**:473 (1990).
9. I. K. Kikoin, A. P. Senchenkov, S. P. Naurzakov, and E. B. Gelman, Preprint IAE-2310, Moscow (1973).
10. V. F. Kozhevnikov, *Zh. Eksp. Teor. Fiz.* **97**:541 (1990) [transl. Sov. Phys. JETF, **70**:298 (1990)]; V. F. Kozhevnikov, S. P. Naurzakov, and A. P. Senchenkov, *J. Moscow Phys. Soc.* **1**:171 (1991).
11. L. J. Duckers and R. G. Ross, *Phys. Lett.* **A38**:291 (1972).
12. F. E. Neale and N. E. Cusack, *J. Phys. F Metal Phys.* **9**:85 (1979).
13. W. Hefner and F. Hensel, *Phys. Rev. Lett.* **48**:1026 (1982).
14. M. Yao, H. Uchtmann, and F. Hensel, *Surface Sci.* **157**:456 (1985).
15. H. Uchtmann, U. Brusius, M. Yao, and F. Hensel, *Z. Phys. Chem. N.F.* **156**:151 (1988).
16. A. Likalter, *Uspekhi Fiz. Nauk* **162**:119 (1992) (in Russian).
17. G. E. Norman and N. Starostin, *Teplofiz. Vysokih Temp.* **8**:413 (1970) (in Russian).
18. L. A. Turkevich and M. H. Cohen, *J. Phys. Chem.* **88**:3751 (1984).
19. K. Suzuki, M. Unitake, and S. Fujiwaka, *IPPJ-310* (Institute of Plasma Physics, Nagoya University, Nagoya, Japan, 1977); K. Suzuki, M. Unitake, S. Fujiwaka, M. Yao, and H. Endo, *J. Phys. Paris* **41**:C8-70 (1980).
20. H. A. Spetzler, M. D. Meyer, and Tin Chan, *High Temp.-High Press.* **7**:481 (1975).
21. M. Hensel, Thesis (University of Marburg, Marburg, 1993).
22. D. I. Arnold, A. M. Gordeenko, P. N. Ermilov, V. F. Kozhevnikov, and S. P. Naurzakov, *Prib. Tekh. Exsp.* No. 5, 143 (1985) (in Russian).
23. N. B. Vargaftik, V. F. Kozhevnikov, A. M. Gordeenko, D. I. Arnold, and S. P. Naurzakov, *Int. J. Thermophys.* **7**:821 (1986).
24. H. McSkimin, *Physical Acoustics—Principles and Methods Vol. IA*, W. P. Mason, ed. (Academic Press, New York, 1964).
25. V. F. Kozhevnikov, D. I. Arnold, and S. P. Naurzakov, *J. Phys. Condenced Matter* **6**:A249 (1994).

26. V. F. Kozhevnikov, S. P. Naurzakov, and D. I. Arnold, *J. Moscow Phys. Soc.* **3**:191 (1993).
27. C. W. Garland, in *Physical Acoustics—Principles and Methods, Vol. VII*, W. P. Mason and R. N. Thurnston, eds. (Academic Press, New York, 1970).
28. L. D. Landau and E. M. Lifshitz, *Hydrodynamics* (Nauka, Moscow, 1986), p. 355.
29. W. W. Warren, Jr., and F. Hensel, *Phys. Rev. B* **26**:5990 (1982).
30. J. Thoen, E. Vangleel, and W. Van Dael, *Physica* **45**:339 (1969).